ACS Sustainable Chemistry & Engineering

pubs.acs.org/journal/ascecg

Research Article

# Techno-Economic Assessment of Sustainable $H_2$ Production and Hydrogenation of Chemicals in a Coupled Photoelectrochemical Device

Xinyi Zhang, Zishuo Li, Lasfitri Rosanty Sinaga, Michael Schwarze, Reinhard Schomäcker, Roel van de Krol, and Fatwa F. Abdi*

Cite This: *ACS Sustainable Chem. Eng.* 2024, 12, 13783−13797

Read Online

ACCESS | Metrics & More | Article Recommendations | Supporting Information



**ABSTRACT:** Photoelectrochemical (PEC) water splitting has been proposed as a promising method to generate sustainable hydrogen, but its competitiveness is hindered by the relatively high cost compared to other generation methods. One strategy to increase the competitiveness of PEC-generated $H_2$ is coupling water splitting with hydrogenation reactions that produce higher-value chemicals. However, the optimal coupled reaction and the energetic and economic benefits of the coupled concept remain uncertain, especially on larger scales. Here, we conduct a comprehensive techno-economic assessment (TEA) of a hypothetical PEC plant with a 1,000 kg $H_2$/day capacity, considering seven potential hydrogenation reactions. The TEA results show that the coupling hydrogenation reaction significantly improves the economic metrics of the system, with acetophenone (ACP) to 1-phenyl ethanol offering the highest returns. Sensitivity analysis shows that solar-to-$H_2$ efficiency and $H_2$-to-chemicals conversion efficiency are the most critical parameters affecting the levelized cost of hydrogen (LCOH) of the system. Finally, benchmark conversions that would result in competitive LCOH values that are comparable to that of fossil fuel based $H_2$ are identified, and the potential impact of these coupled PEC hydrogenation reactions on the global $H_2$ market is discussed.

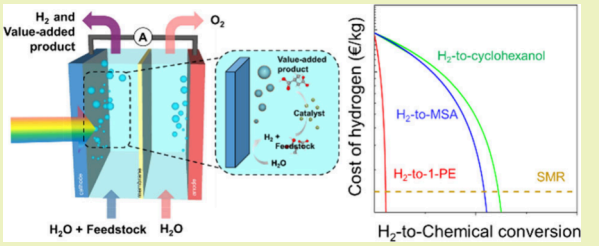


**KEYWORDS:** *techno-economic assessment, water splitting, green chemical synthesis, green hydrogen, coupled catalysis, hydrogenation, (photo)electrochemistry*

## INTRODUCTION

In response to the worsening impact of global warming, 195 parties (194 states plus the European Union) have joined the Paris Agreement, and most have pledged to accomplish their carbon neutrality goal by 2050.[1] A key action point is to integrate more renewable sources into the energy system, replacing fossil sources. However, most renewable sources are intermittent and diluted. The rapid growth of renewable energy capacity, especially solar and wind, will likely lead to challenges in energy supply reliability.[2] Hydrogen, a carbon-free molecule with a high gravimetric energy density, has been widely considered an important operating reserve to compensate for the surplus and shortages of energy systems. Notably, hydrogen is also an essential feedstock being widely used in the refining, chemical, and steel industries.[3] Unfortunately, the current hydrogen supply is almost entirely produced with fossil fuel-based processes, primarily via steam methane reforming (SMR), resulting in the annual consumption of 205 billion $m^3$ of natural gas and the emission of 820 Mt $CO_2$.[4] In 2021, less than 0.1% of the $H_2$ produced today is "green",[3] mainly through wind- and PV-powered water electrolysis. Several demonstrations of integrated photoelectrochemical (PEC) water splitting devices, in which sunlight absorption and electrolysis of water are combined in a single unit, have also been reported with solar-to-hydrogen (STH) efficiencies approaching 20% for small-area devices.[5,6] Compared with PV-powered electrolysis, this configuration offers two potential advantages. One is the close thermal coupling between the absorber, catalyst, and electrolyte solution, which improves the electrochemical reaction kinetics and increases the efficiency of the light absorber by cooling. Furthermore, PEC devices operate at 1−2 orders of magnitude lower current densities (10−20 mA/$cm^2$), which enables the use of abundant, nonplatinum group electrocatalysts.[7]

Despite the promising potential of PEC-produced hydrogen, several techno-economic analyses (TEAs) and net energy assessments (NEAs) have shown that the approach is still not energetically and economically competitive for large-scale implementation. The levelized cost of hydrogen (LCOH)

Received: April 25, 2024
Revised: August 23, 2024
Accepted: August 26, 2024
Published: September 3, 2024

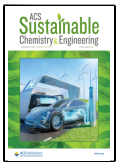

**Table 1. Substrates (Feedstocks) and the Corresponding Products of Seven Hydrogenation Reactions Considered in This Study**[a]

| Substrate/Feedstock | Product | Reaction | ref |
|---|---|---|---|
| Itaconic acid | Methylsuccinic acid | $C_5H_6O_4 + H_2 \rightarrow C_5H_8O_4$ | 13,22 |
| Levulinic acid | Valeric acid | $C_5H_8O_3 + 2H_2 \rightarrow C_5H_{10}O_2 + H_2O$ | 23,24 |
| Levulinic acid | γ-Valerolactone | $C_5H_8O_3 + H_2 \rightarrow C_5H_8O_2 + H_2O$ | 25,26 |
| Phenol | Cyclohexanol | $C_6H_6O + 3H_2 \rightarrow C_6H_{12}O$ | 23,27 |
| Acetophenone | 1-Phenylethanol | $C_8H_8O + H_2 \rightarrow C_8H_{10}O$ | 23,28 |
| Carbon dioxide | Ethylene | $2CO_2 + 6H_2 \rightarrow C_2H_4 + 4H_2O$ | 29,30 |
| Carbon dioxide | Oxalic acid | $2CO_2 + H_2 \rightarrow (COOH)_2$ | 29,31 |

[a]The chemical structures of these substrates and products are shown in Table S2.

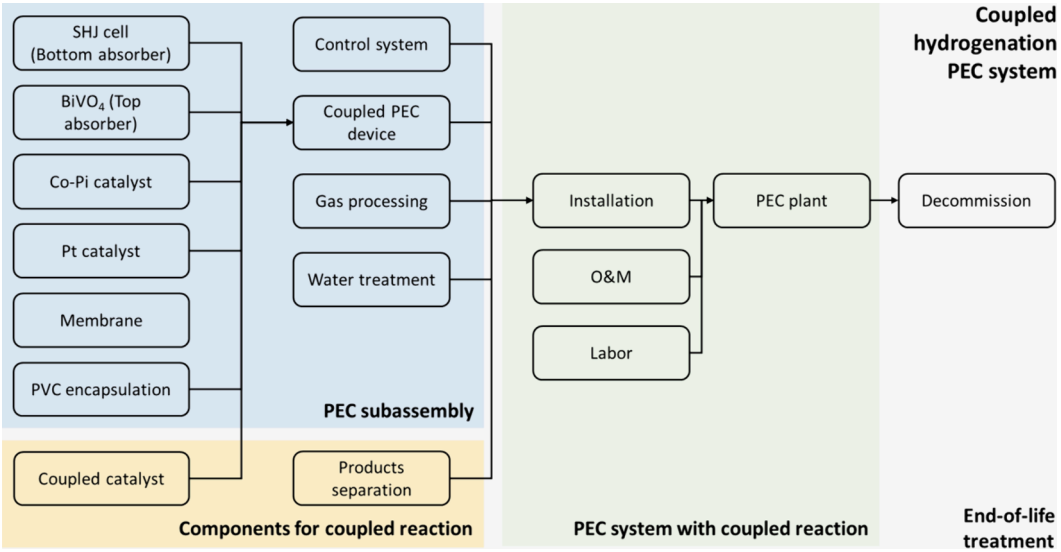


**Figure 1.** Block diagram of the "cradle-to-gate" system boundary of the coupled PEC hydrogenation system considered in this study.

originating from PEC systems has been estimated at ∼9.6−10 €/kg $H_2$.[8,9] This LCOH is significantly higher than that of SMR-produced $H_2$ (1.5 €/kg $H_2$).[10] PEC produced hydrogen is not economically attractive even when the current market price for green hydrogen is considered (9.16 €/kg[11] for green $H_2$ vs 1.5−6 €/kg for gray hydrogen).[12] In fact, other than theoretical large scale biomass gasification, which is predicted to have an LCOH as low as 1.3 €/kg if successfully realized, the LCOHs of other $H_2$ production technologies are all higher than that of SMR-produced $H_2$ (see Table S1).

One approach to increasing the competitiveness of PEC-generated $H_2$ is to directly integrate successive utilization of $H_2$ within the same PEC devices. The integration of the hydrogen production and utilization processes further reduces the total system costs, and if the successive utilization yields valuable chemicals, the overall competitiveness of the PEC device can be improved. For example, we recently demonstrated the concept of coupling PEC $H_2$ production with the homogeneous hydrogenation of biomass feedstock in a single reactor.[13] In that report, the hydrogenation of itaconic acid (IA) to methylsuccinic acid (MSA), a valuable chemical compound that finds applications in cosmetics,[14] polymer synthesis,[15] and powder coating,[16] was chosen as the hydrogenation reaction of interest. Due to the well-matched kinetics of the PEC and the room-temperature hydrogenation processes, a coupling efficiency ($H_2$-to-MSA conversion) beyond 50% was experimentally demonstrated. Based on this demonstration, a life cycle net energy balance assessment was conducted and showed that $H_2$ produced by this coupled PEC device has a lower cumulative energy demand (CED) than SMR-produced $H_2$.[17] A techno-economic assessment based on a projected 100 $m^2$-scale device was also performed, and the expected profitability of the concept was reported.[13]

In this study, we extend the scale of the techno-economic assessment to a coupled PEC hydrogenation plant generating the equivalent of 1,000 kg $H_2$/day (and the equivalent hydrogenation product). As target hydrogenation reactions, we consider the previously reported hydrogenation of IA to MSA and six additional hydrogenation reactions that have been reported to occur at or close to room temperature and pressure. These reactions are listed in Table 1. The substrates considered are biomass-derived feedstocks that can be mass-produced sustainably, such as IA,[18] levulinic acid (LA),[19] phenol,[20] and acetophenone,[21] and $CO_2$. The corresponding products all find use in various industrial-scale chemical processes and applications. We use several techno-economic metrics to elaborate on the benefits, if any, of coupling these hydrogenation reactions to PEC water splitting within a single device. Finally, the economic performance of the coupled processes is compared with the benchmark figures of conventional SMR hydrogen to assess the implementation potential of the coupled reactions.


https://doi.org/10.1021/acssuschemeng.4c03463
ACS Sustainable Chem. Eng. 2024, 12, 13783−13797

## METHODOLOGY

We followed the principles and framework of Techno-Economic Assessment & Life Cycle Assessment (LCA) Guidelines for $CO_2$ Utilization (Version 1.1) established by the Global $CO_2$ Initiative.[32] The guidelines provide a specific protocol for multifunctional carbon capture and utilization (CCU) plants, which was adapted for the PEC system in this study. The PEC-produced hydrogen and hydrogenated chemicals in this study were assumed to be free of downstream emission after leaving the plant gate, i.e., this work adopted a "cradle-to-gate" system boundary that includes all costs related to raw materials, product manufacturing, and decommissioning. Since the scale of the PEC plant considered here is much smaller than the market volumes of hydrogen and the hydrogenated chemicals, the productivity of the prospective PEC system was assumed to not impose any market disturbance. Like previous works, the scrap value and disposal of the system were not considered.[9,33] Figure 1 shows the cradle-to-gate boundary that was used for this TEA.

The engineering design of the plant scale system used in this study was based on the information retrieved from the US Department of Energy (DOE) Task 5.1 report on techno-economic analysis of PEC hydrogen production.[33] Certain technical design aspects were modified to reflect that our PEC process is coupled to a catalytic hydrogenation reaction, and several parameters were updated to reflect the geographical and temporal data that are relevant to Europe, such as solar resource data obtained from EU Science Hub Photovoltaic Geographical Information System in 2022,[34,35] water and electricity tariff in Europe, and market prices for precious metals.[36] In this assessment, the electricity consumed for system operation is assumed to be delivered from the German electricity grid which has a mix of power sources, i.e., renewable and nonrenewable. In 2023, renewables accounted for about 60% of the electricity generation in Germany.[37]

**Economic Metrics.** A range of economic metrics as system performance indicators were calculated based on the system input and outputs flows. Net present value (NPV) describes the current profitability of a system, considering its initial capital investment and future generated cash flows. A negative NPV indicates that a project will not be profitable and vice versa. Conditions with zero NPV therefore define the break-even point of the system. Here, capital investments were made during the base year (2023). Cash flows were assumed to start in the following year, and they were discounted to the base year using the following equation:

$$\mathrm{NPV} = \sum_{i=1}^{n} \frac{\mathrm{CF}_i}{(1+r)^{i-1}} - \mathrm{Capex} - \sum_{i=1}^{n} \frac{\mathrm{Opex}_i}{(1+r)^{i-1}} - \frac{\mathrm{Decom\_ex}}{(1+r)^n} \quad (1)$$

$\mathrm{CF}_i$ is the income cash flow or annual revenue in the operation year $i$, Capex is the capital investment (including direct and indirect capital cost), $\mathrm{Opex}_i$ is the operation cost in the year $i$, Decom_ex is the decommissioning cost, $n$ is the system lifetime (base = 20 years), and $r$ is the real discount rate (4.34%) based on nominal yields and inflation expectations from analyst surveys.[38]

The $\mathrm{CF}_i$ of the system was calculated by taking the sum of the annual revenues from $H_2$ ($\mathrm{CF}_{H_2,i}$) and the hydrogenation products ($\mathrm{CF}_{\mathrm{hydrogenation},i}$).

$$\mathrm{CF}_i = \mathrm{CF}_{H_2,i} + \mathrm{CF}_{\mathrm{hydrogenation},i} \quad (2)$$

$$\mathrm{CF}_{H_2,i} = \Phi_{H_2\_\mathrm{collected},i} \times \mathrm{SP}_{H_2} \quad (3)$$

$$\mathrm{CF}_{\mathrm{hydrogenation},i} = \Phi_{\mathrm{hydrogenation},i} \times \mathrm{SP}_{\mathrm{hydrogenation}} \quad (4)$$

$\Phi_{H_2\_\mathrm{collected},i}$ and $\Phi_{\mathrm{hydrogenation},i}$ are the amounts of $H_2$ and hydrogenation products (in kg) collected annually in year $i$, respectively (see the section below: "Description and Assumptions of the PEC Facility"). $\mathrm{SP}_{H_2}$ and $\mathrm{SP}_{\mathrm{hydrogenation}}$ are the selling price of $H_2$ and hydrogenation products, respectively. The selling price is assumed to be constant throughout the system's lifetime. There is currently a considerable spread of $H_2$ prices depending on the "color" of $H_2$ (green vs gray), from 1.4 €/kg ($H_2$ from SMR)[10] to 11.6 €/kg (green $H_2$ from renewable grid powered electrolysis).[39] A very optimiztic expectation was made by a Canada-based company H2 V Energies who are planning to supply green hydrogen in 2022 at prices of 2.4 €/kg[40,41] (although the project has been postponed to start operation in 2026).[42] In this study, we assumed the benchmark market price of hydrogen to be 2.5 €/kg.

Table S3 lists the current market prices of the hydrogenation feedstocks and products considered here. We note that the market price data for industrially produced MSA is lacking, and that the current market price of high purity MSA compound from laboratory synthesis is extremely expensive.[43,44] Therefore, like our previous study,[13,45] the market price of mass-produced MSA was estimated based on the energy demand of its manufacturing. Our previous life-cycle net energy balance study reported that the energy demand for conventional production of MSA is ~10 times higher than that for IA.[17] Therefore, MSA is assumed to be 10 times more expensive than IA, using the energy demand relationship coefficient between them. It is therefore understood that the absolute number in our TEA of MSA should therefore be considered as a preliminary estimation and that the observed trends and sensitivity analysis should be interpreted accordingly.

The internal rate of return (IRR) is the real discount rate at which the NPV = 0. It is the minimal value of the annualized interest rate at which the initial capital investment must grow to breakeven the total cost.[46] If the IRR of a project is higher than the discounted rate or that of other projects, then the project is considered more competitive. We calculated the IRR using MATLAB by setting the left-hand side of eq 1 to zero and solving for $r$. The payback time (PBT) in unit of year represents the time required to recoup the total expenditure, which is defined as follows:

$$\mathrm{PBT} = \frac{\mathrm{Capex} + \sum_{i=1}^{n} \frac{\mathrm{Opex}_i}{(1+r)^i} + \frac{\mathrm{Decom\_ex}}{(1+r)^n}}{\overline{\mathrm{CF}}} \quad (5)$$

$\overline{CF}$ is the average annual revenue:

$$\overline{\mathrm{CF}} = \frac{\sum_{i=1}^{n} \frac{\mathrm{CF}_i}{(1+r)^i}}{n} \quad (6)$$

The levelized cost of hydrogen (LCOH) indicates the minimal selling price of $H_2$, in units of €/kg, that would be required to cover the system cost during the entire construction, operation, and decommission period. Since the coupled PEC hydrogenation system is a multifunctional system with two output product flows, we calculated the LCOH by


https://doi.org/10.1021/acssuschemeng.4c03463
ACS Sustainable Chem. Eng. 2024, 12, 13783−13797

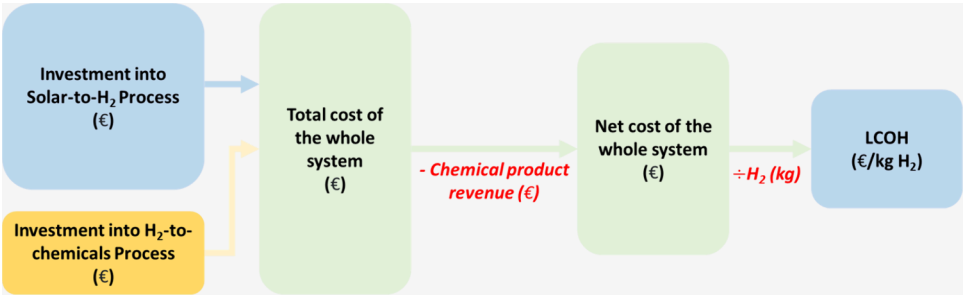


**Figure 2.** Cost allocation approaches within the multifunctionality coupled PEC hydrogenation system considered in this study. The cost attributed to $H_2$ is calculated based on the net cost after subtracting the revenue from the hydrogenated products.

taking the revenue from the hydrogenation products to compensate the cost of system.[47] The cost flow approach is shown in Figure 2. A negative LCOH is possible as a consequence of this approach and indicates that the product revenue from the hydrogenation products is higher than the overall cost of the system. The following equation shows how LCOH is calculated:

$$\text{LCOH} = \frac{\text{Capex} + \sum_{i=1}^{n} \frac{\text{Opex}_i}{(1+r)^i} + \frac{\text{Decom\_ex}}{(1+r)^n} - \sum_{i=1}^{n} \frac{\text{CF}_{\text{hydrogenation},i}}{(1+r)^i}}{\sum_{i=1}^{n} \frac{\Phi_{\text{H2\_collected},i}}{(1+r)^i}} \quad (7)$$

**Description and Assumptions of the PEC Facility.** The base case scenario of the PEC facility in this study is the following: (i) a STH efficiency of 10%, (ii) lifetime of 20 years, (iii) area capacity factor ($\phi$) of 90% (i.e., 90% of the panels are converting solar energy to $H_2$ on an average day),[48] and (iv) a $H_2$-to-chemicals conversion (*vide infra*) of 10% (only when the system includes coupled hydrogenation). Table S4 lists all of the parameters assumed in the base case scenario. Our study considered a hypothetical large-scale PEC facility with a production capacity of 1,000 kg $H_2$/day. The fixed flat panel array design was adapted from the Type 3 PEC configuration described by James et al.[33] in their TEA report. We have chosen the Type 3 panel configuration as it represents a compromise between the simpler colloidal suspension configurations (Types 1 and 2) with lower demonstrated efficiencies vs the more efficient and more complex configuration with tracking solar concentrator (Type 4). Additionally, the existence of other LCA and TEA studies based on Type 3 configuration facilitates the comparison between our coupled PEC system and previous studies.[49] The PEC fixed planar array is inclined at the optimum tilt angle (constant throughout the year), and each panel is made up of multiple cells. The construction of the PEC device is based on our recently reported 50 $cm^2$ demonstration devices.[50] It comprises the following components required for unassisted solar water splitting: a $BiVO_4$ top absorber, a silicon heterojunction (SHJ) bottom absorber, a deposited platinum catalyst, an ion exchange membrane, as well as separate inlets and outlets.[17] For simplicity, it is assumed that the Pt catalyst deposited on the solar-grade fluorine-doped tin oxide (FTO) coated glass is sufficiently thin to allow sunlight transmission without incurring optical loss.[51,52] While this assumption may not be entirely precise from a device operation standpoint and alternative geometrical configurations might be employed, this factor does not significantly affect the overall analysis in this techno-economic assessment TEA study. Figure 3a shows the schematic configuration of the PEC device, with the

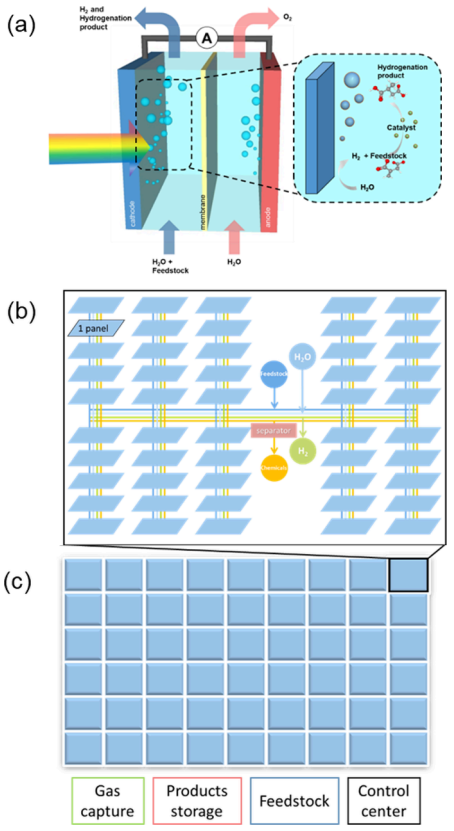


**Figure 3.** Schematic illustration of the 1,000 kg $H_2$/day production PEC system at different levels. (a) Photoelectrochemical cell with coupled hydrogenation. $H_2$ generated at the cathode is utilized directly to hydrogenate feedstock to a valuable product with the help of homogeneous catalyst dispersed in the catholyte. (b) PEC array layout. (c) Facility layout.

homogeneous catalyst dissolved in the catholyte (1 M potassium phosphate is the supporting electrolyte). Inside the cell, the coupled hydrogenation reaction takes place in the catholyte compartment, where the generated $H_2$ is utilized to hydrogenate substrates to valuable chemical products with the assistance of the homogeneous catalyst. For all the investigated coupled hydrogenation reactions, we consider the same homogeneous catalyst, Rh-TPPTS, which is used and dissolved in the catholyte solution with the same concentration. While each reaction realistically would use a different catalyst and different concentration, this assumption is made to simplify the


https://doi.org/10.1021/acssuschemeng.4c03463
ACS Sustainable Chem. Eng. 2024, 12, 13783−13797

calculation since the resulted economic metrics are not sensitive to the catalyst cost, i.e., the contribution from this parameter is negligible. A constant 1% annual degradation rate of the device is assumed over its entire operational lifetime. This assumption regarding the stability of $BiVO_4$ is highly optimiztic, which is made to enable longevity over a few years for this preliminary assessment. Currently, the highest stability of $BiVO_4$, as reported by Kuang et al., demonstrates operation for over 1100 h with minimal degradation or performance loss. A longer lifetime is expected to be demonstrated by $BiVO_4$ or other PEC electrode materials so that future industrial deployment of large-scale water splitting in the future can be realized.[53]

Figure 3b,c shows the baseline system layout which has a total 118,778 $m^2$ capture area (corresponding to 59,389 panels of 1 × 2 $m^2$ and 60 fields each containing approximately 1,000 panels), while 10% of the capture area is assumed to be inactive.[33,54] Although the size of a single cell will not affect the overall cost evaluation of a panel, a panel is assumed to consist of multiple PEC cells of 50−100 $cm^2$ as this is the largest size of a single cell being reported to date.[50] The annual amount of hydrogen produced by the PEC system ($\Phi_{H_2\_produced,i}$ in kg) is determined by the device performance and operational parameters:

$$\Phi_{H_2\_produced,i} = \frac{\Phi_{sunlight} \times \eta_{STH} \times 365 \times A_{active} \times \phi}{LHV_{H_2}} \quad (8)$$

$\Phi_{sunlight}$ is the solar intensity (3.43 kWh/$m^2$/day, an average value over the whole year), $\eta_{STH}$ is the STH efficiency, $A_{active}$ is the active area, $\Phi$ is the system area capacity factor (90% for base case), and $LHV_{H_2}$ is the lower heating value of $H_2$ (33 kWh/kg or 120 MJ/kg).

Considering that the hydrogenation reaction may not convert all the in situ generated $H_2$ to value-added products, a term of $H_2$-to-chemicals conversion ($\mu$), which ranges from 0% to 60%, was introduced in the different assessment scenarios. The annual amount of $H_2$ consumed ($\Phi_{H_2\ consumed,i}$)) in the reaction is therefore a product of $\mu$ and the annual amount of $H_2$ produced on the cathode ($\Phi_{H_2produced,i}$):

$$\Phi_{H_2\_consumed,i} = \mu \times \Phi_{H_2\_produced,i} \quad (9)$$

The annual amount of $H_2$ collected after the reaction ($\Phi_{H_2collected,i}$) is

$$\Phi_{H_2\_collected,i} = (1 - \mu) \times \Phi_{H_2\_produced,i} \quad (10)$$

The annual amount of hydrogenation products generated ($\Phi_{hydrogenation,i}$) and feedstocks consumed ($\Phi_{feedstock,i}$) can therefore be determined:

$$\Phi_{hydrogenation,i} = \frac{\Phi_{H_2\_consumed,i}}{M_{H_2}} \times M_{hydrogenation} \times \frac{\nu_{hydrogenation}}{\nu_{H_2}} \quad (11)$$

$$\Phi_{feedstock} = \frac{\Phi_{H_2\_consumed,i}}{M_{H_2}} \times M_{feedstock} \times \frac{\nu_{feedstock}}{\nu_{H_2}} \quad (12)$$

$M_{H_2}$, $M_{hydrogenation}$, and $M_{feedstock}$ are the molecular masses of $H_2$, the hydrogenation product and the feedstock, respectively. $\nu_{H_2}$, $\nu_{hydrogenation}$, and $\nu_{feedstock}$ are the stoichiometry coefficients for $H_2$, the hydrogenation product and the feedstock, respectively, as shown in Table 1.

The total facility cost consists of the capital cost (direct and indirect), the operational and maintenance (O&M) cost and the decommissioning cost. The direct capital cost includes the PEC reactor cost, the balance of system (BOS) cost, and the installation cost; the detailed contributions are discussed in the "System Components and Costs" section. Additional indirect capital cost is considered in this study, and the amount is 27% of the direct capital cost (7% for engineering design and 20% for process contingency budget).[33] The cost of operation and maintenance includes the feedstock cost, utility cost, replacement cost, fixed maintenance cost, and labor cost. Feedstock inventories adhere to the mass balance and are affected by the production efficiency and delivery distance. Utility cost is estimated based on the equipment's power rating and operating load. Replacement of major components and fixed maintenance are assumed to cost 12% and 2.8% of the total capital cost, respectively, based on the performance data from several electrolyzer companies.[55] Labor cost during the operation time is estimated based on the average engineering labor cost in Europe[56] and a utility PV power generation plant having 80 permanent employees for 400,000 solar panels with a linear integration.[57] The decommissioning cost is assumed as 10% of the initial capital cost.[33] Due to the relatively low technological readiness level (TRL) of PEC water splitting, industrialized mass production of PEC device components is not yet available. Scaling up of the manufacturing process was therefore calculated assuming an additional investments into manufacturing tools at 1.5% of the total capital cost.[33]

**System Components and Costs.** *PEC Reactor Subassembly.* Real-time market prices during this study (2022−2023) were used to determine the costs of the raw materials. The amount of material usage and the manufacturing cost for the individual components were calculated based on the experimental data and literature. The cost of the tools was translated into the equivalent cost per unit area by dividing the purchase price with the total product yields. The primary expenditure of PEC cell, $Ex_{cell}$, is calculated based on a bottom-up approach from the cost of each part and subpart.

$$Ex_{cell} = \sum P_{material} \times W_{material} + \sum P_{utility} \times W_{utility} + Ex_{equipment} + Ex_{labor} \quad (13)$$

$P_{material}$ is the cost of raw materials in units of €/g, $W_{material}$ is the amount of material used in units of gram/$m^2$, $P_{utility}$ is the electricity or water tariff[58,59] of the region in units of €/kWh and €/$m^3$, respectively, $W_{utility}$ is the amount of electricity and water used in units of kWh/$m^2$ and $m^3$/$m^2$, $Ex_{equipment}$ is the equivalent cost of purchasing the equipment to produce unit area of cell over its entire lifetime in units of €/$m^2$, and $Ex_{labor}$ are the labor costs for manufacturing the cell in units of €/$m^2$.

The coupled PEC device investigated in this study adopted a silicon heterojunction (SHJ) cell without front metal contacts as the bottom absorber. Louwen et al.[60] reported a 0.34 €/$W_{peak}$ production cost for SHJ cell in their TEA. We adapted this figure to a single-sided metallized SHJ cell by removing half of the materials and energy consumed in the metallization process.

The $BiVO_4$-based photoanode top absorber is deposited directly on the ITO layer of the SHJ cell. This avoids the need for additional glass substrates and reduces the complexity of


https://doi.org/10.1021/acssuschemeng.4c03463
ACS Sustainable Chem. Eng. 2024, 12, 13783−13797

the device. The material consumption and the fabrication steps considered were obtained from our previous report on spray-pyrolyzed $BiVO_4$.[61] Currently, there are no data available for industrial scale fabrication of the $BiVO_4$ layer. Thus, the cost was estimated based on the laboratory-scale fabrication process performed at the Institute for Solar Fuels, Helmholtz-Zentrum Berlin, by introducing a scaling factor, as mentioned in the previous section.

The oxygen and hydrogen evolution catalysts, i.e., cobalt phosphate ($Co-P_i$) and Pt, are electrodeposited onto $BiVO_4$ and solar grade glass, respectively. The electrodeposition energy usage for thin film coatings has been reported as 1.54 $kWh/m^2$,[62] which includes dipping (0.125 $kWh/m^2/min$), rinsing, drying and calcination steps. In our electrodeposition process, only a 15 min dipping treatment is involved. The estimated primary energy requirements for the electrodeposition of $Co-P_i$ and Pt are 20.1 and 13 $MJ/m^2$, respectively.[52]

Nafion is considered as the ion conducting and gas impermeable membrane, and the cost was estimated based on the average market price of 240 €/$m^2$.[9] The encapsulation consists of a transparent glass cover and a PVC chassis. The costs associated with ancillary processes (i.e., miscellaneous chemicals,[63] water pumping and cleaning,[64] environmental control of the manufacturing facilities)[65] for device manufacturing were disaggregated from PV related LCA studies. The PEC reactor subassembly also includes feedwater pumps and manifold poly vinyl chloride (PVC) pipes, which deliver electrolytes and liquid products between the feedstock point, individual reactors, the gas collection unit, and products separation unit. The length of different sizes of pipes were recalculated based on the value from the DOE report.[33] Finally, the installation of the PEC reactor on site is assumed to cost 20 €/panel.[33] The detailed values of materials and energy use for fabricating and installing the PEC reactor are listed in Table S5.

*Balance of System (BOS).* The daily water supply is assumed to be provided by a water treatment facility working based on the reverse osmosis/electrodeionization (RO/EDI) method is assumed for daily water supply.[66,67] The capacity rating needs to cover the peak water flow rate of 2 $m^3$/hour for the whole system.[48] As the major feedstock, the water supply for PEC production needs to be of high purity (resistivity > 1 MΩ cm at 25 °C) with minimum ion concentration to avoid contamination of the electrochemically active surfaces. By utilizing the RO/EDI technique, feed water is first treated by RO and then undergoes EDI for deionization. This process is best suited for chemical-free operation. The cost for utility, chemicals, and other consumables used during the RO/EDI process was accounted for in the O&M cost section.[66] Waste management of the RO concentrate was also considered which leads to an additional €0.35/$m^3$ of total treated water.[68] Water usage during the $H_2$ production process was based on stoichiometric amount requirements and an additional 1% evaporation factor. Additional water consumption for cleaning of the panel surface was assumed to be 25 L/year/$m^2$ based on data from a utility scale PV system.[69]

Water pumps for the reactors are assumed to run only during $H_2$ production and for several hours after the $H_2$ production period is over. The water feed can be handled with industrial electric water pumps,[70] whose energy consumption is estimated from values reported by Plappally et al.[71]

A gas handling system that includes PVC piping, a two-stage gas compressor, and a condenser/cooler is used to collect, compress, separate, and deliver the $H_2$ gas produced to the collection station/pipeline. The $H_2$ gas at the outlet of the PEC device is at atmospheric pressure and pressurized to 300 psi (20.6 bar) before being transferred to the collection station/pipeline. The compressor capacity was dimensioned based on the peak annual $H_2$ production, i.e., highest solar irradiance. On all other days, the compressor operates only at reduced capacity. The condenser/cooler unit reduces the gas temperature and removes water vapor before feeding into the compressor. The cost of all the gas handling equipment was derived from previous works.[33]

Control automation is assumed to be realized with LabVIEW software,[72] programmable logic controllers (PLCs),[73] and office computers.[74] The cost of these monitor and control tools was adapted from a previous report.[33] The installation of all BOS components was estimated as 30% of their initial capital cost.[33] The detailed parameters and costs of BOS are shown in Table S6.

*Components for $H_2$-to-Chemicals Processes.* One major component of the hydrogenation reaction is the feedstock. In this study, there are several feedstocks, and depending on the locations of the source, different transport distances of feedstocks need to be considered. In this study, the base case distance from the source of the feedstock to the site is assumed to be 100 km. The delivery cost is then calculated separately for different delivery approaches, i.e., pipeline transport for $CO_2$ and truck or railway transport for solid feedstock. As reported in previous studies, the cost of $CO_2$ transportation varies between US$4−45/$tCO_2$.[75] For solid and liquid feedstocks, i.e., itaconic acid, levulinic acid, phenol and acetophenone, a delivery cost of €0.375−0.395/tkm by truck or €0.203−0.246/tkm with truck plus trailers was considered.[76] Since the delivery cost is not significant, we included this in the feedstock cost category.

Before feeding the catholyte into the PEC reactor, the feedstocks in their solid, liquid or gas form and the Rh-TPPTS catalyst need to be dissolved in a continuous stirred tank reactor (CSTR).[77] The electricity consumption of CSTR units is derived from the power rating of the equipment.[78] During the coupling reaction, the feedstock consumption is calculated based on the stoichiometric relationship between feedstocks and hydrogen as shown in Table 1 and the $H_2$-to-chemicals conversion efficiency.

Rh-TPPTS with a 0.9 mM concentration is prepared and utilized as the homogeneous catalyst for the hydrogenation reaction. Ideally, as a catalyst, Rh-TPPTS would not be consumed during the chemical reaction. However, this is not realistic in practical production activities; a 1.2% annual loss is assumed, which corresponds to the replacement rate of the PEC reactor.

After the coupled hydrogenation reaction takes place in the PEC reactor units and reaching the preset conversion efficiency (by controlling the flow rate),[21] a mixture of catholyte, feedstocks, Rh-TPPTS, $H_2$ gas, and hydrogenation products is delivered to a separation facility. Compressed $H_2$ gas is collected and delivered to pipelines, and the rest of the liquid solution is sent to a separation unit for chemical products extraction. The separation process of succinic acid from the typical mixture produced during the conventional fermentation process was used as a proxy process for base case chemical separation.[79] The produced mixture of feedstocks,


https://doi.org/10.1021/acssuschemeng.4c03463
ACS Sustainable Chem. Eng. 2024, 12, 13783−13797

hydrogenation product, $H_2O$, and catalyst are centrifuged. The mixture of the remaining feedstocks, $H_2O$, and catalyst is recycled to the PEC device, and the hydrogenation product solution is fed to adsorption/desorption columns. After every three cycles, the adsorption/desorption column is exposed to hot air to remove contaminants. This liquid is further concentrated in an evaporator and the concentrated liquid is fed to a continuous crystallizer. Purified hydrogenated chemical products are then produced after filtration and drying and will be stored in airtight containers. The base case separation flow (the separation of succinic acid) of the hydrogenation product is illustrated in Figure S1. The detailed costs for additional components needed to perform the coupled hydrogenation process are given in Table S7. The separation processes of cyclohexanol and oxalic acid were also considered to provide a more comprehensive cost evaluation of the separation process. For example, Wang et al. have designed and evaluated an energy-saving industrial distillation processes for separating cyclohexanol,[80] which costs US$4.2−6 million/year for a working load of 30,400 kg/hour. This translates to 138.02 €/$m^2$ considering the design of our evaluated PEC system. For oxalic acid separation, the liquid−liquid extraction (LLE) technique has been reported to account for 9% of the whole operation cost in a $CO_2$ capture and reduction system,[31] which equals to 411.3 €/$m^2$. This range of separation cost was considered for our sensitivity analysis.

## RESULTS AND DISCUSSION

We first analyze the cost of the system according to the approach and boundary conditions described in the "Methodology" section. For the base-case assumptions, the total capital expense for the coupled PEC hydrogenation system was found to be €71.6 million, which translates to 603 €/$m^2$. Figure 4 shows the cost breakdown of the system. The PEC device accounted for 77.8% of the total capital cost. Within the PEC device, the Nafion membrane is the most cost intensive component, contributing to 42.8% of the total capital cost. This is not entirely surprising due to the high cost of Nafion (240 €/$m^2$). It is noted that James et al. expected the cost of Nafion membrane to be reduced to 32.2 €/$m^2$ in their TEA study due to mass production,[81] but the current market price is still much more expensive. The costs of the SHJ cell and the BiVO4 follow behind with values of 13.9% and 9.3% of the total capital cost, respectively. Interestingly, platinum and the Rh/TPPTS catalyst, which are or contain expensive noble metals, contribute only 0.8% and 1% of the capital cost, respectively. This is because of their very limited use in the coupled PEC hydrogenation system. The separation unit is the most cost intensive component in the BOS (12.5%), followed by installation costs (6.8%). Other BOS costs, i.e., gas processing facilities, water treatment facilities, and control systems, do not contribute much to the total capital cost. As a comparison, Figure S2 shows the cost breakdown of the same PEC system but when only $H_2$ production is considered. A similar distribution can be observed except for the absence of the homogeneous catalyst and the components for the separation of the hydrogenation products.

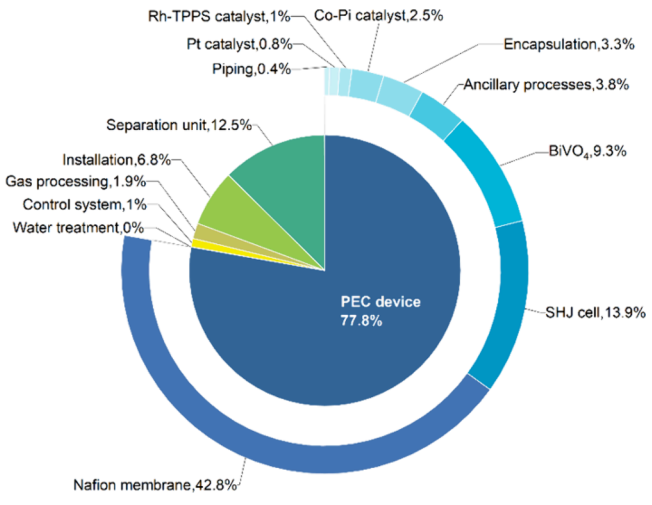


**Figure 4.** Percentage breakdown of the direct capital cost for a coupled PEC hydrogenation system. As a comparison, the cost breakdown for a PEC system that generates only $H_2$ is shown in Figure S2.

The finding that the PEC device is the largest contributor to the majority portion of the total capital cost is consistent with our recent net energy assessment.[17] In that study, the PEC device was also reported to have the highest cumulative energy demand among the other components. However, the SHJ cell was identified as the most energy intensive component of the device, while Nafion is here found to be the most cost intensive component in the current TEA study. Although the production of SHJ cell consumes a lot of energy, the material cost is much lower than that of Nafion. These results illustrate the importance of both energy and economic assessments in the evaluation of a system.

Figure 5a shows the annual O&M cost for the seven PEC coupled hydrogenation systems (under the base case scenario) as well as the case without coupled hydrogenation (i.e., only $H_2$ production). When only hydrogen is produced, the annual O&M cost is 32.8 €/$m^2$. All PEC systems with coupled hydrogenation require higher O&M cost than the noncoupled PEC system, due to the additional substrate feedstock and separation costs. The O&M cost for the coupled system producing 1-phenylethanol (1-PE) is the highest, ∼12 times that of producing only $H_2$. The main cost driver is the feedstock acetophenone (ACP), which is a relatively expensive substrate chemical compared to other feedstocks. The coupled system that generates MSA shows ∼4 times higher O&M cost compared to the noncoupled system; again, feedstock cost is the main cost driver as IA is the second most expensive feedstock considered. When the feedstock prices are the same, i.e., for valeric acid (VA) vs $\gamma$-valerolactone (GVL) and ethylene vs oxalic acid (OA), the O&M cost differences are simply attributed to the stoichiometric difference between $H_2$ and the hydrogenation products in the respective reactions (since the percentage of the separation costs are assumed to be identical for the different products).

The distribution of system components for the three selected hydrogenation products is shown in Figure 5b-d. As shown in Figure 5b, IA feedstock into the $H_2$-to-MSA process (29.5%) and separation process (59.7%) are the two main cost drivers of the total O&M cost (121.5 €/$m^2$). The main reason is that the annual yield of MSA in terms of weight is the highest among all hydrogenation products and the separation process is linearly dependent on the weight of the products. Fixed maintenance accounts for 7.2% of the total cost, with the remaining 3.7% made up of labor, device replacement, electricity, delivery of feedstock, and water. For cyclohexanol production (Figure 5c), the costs of different components are


https://doi.org/10.1021/acssuschemeng.4c03463
ACS Sustainable Chem. Eng. 2024, 12, 13783−13797

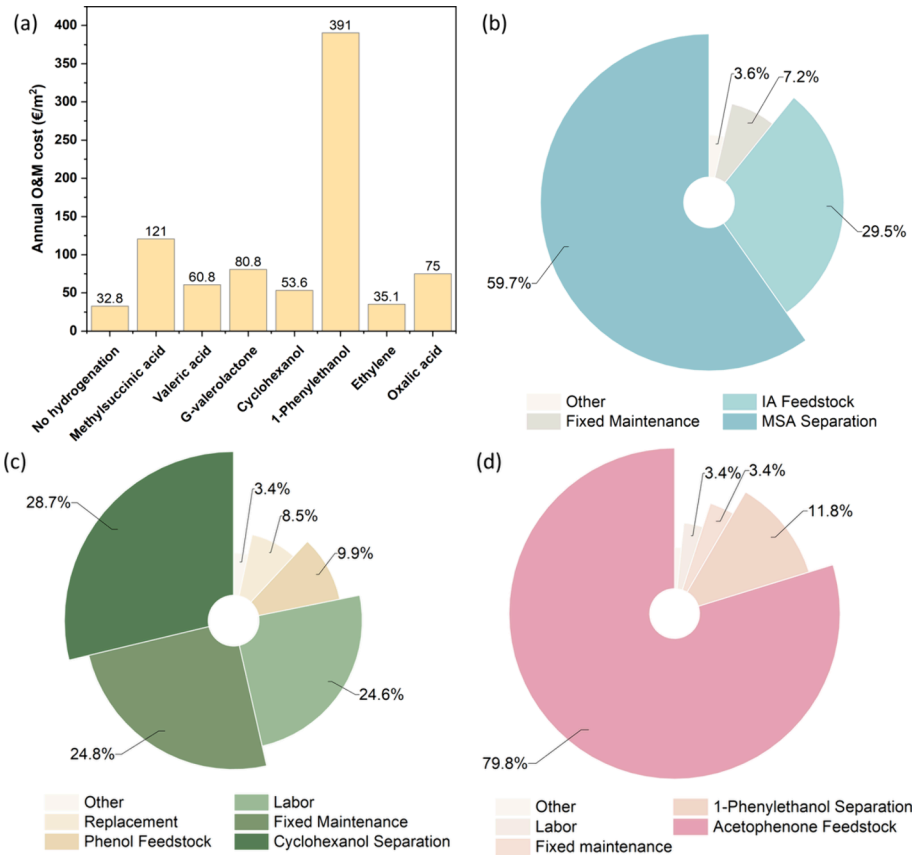


**Figure 5.** Annual O&M cost breakdown of PEC systems. (a) Cost breakdown for all PEC productions, including a system that produces only $H_2$ (i.e., no hydrogenation) and coupled PEC hydrogenation systems that produce seven hydrogenation products. Cost breakdown of coupled hydrogenation products: (b) MSA, (c) cyclohexanol, and (d) 1-phenylethanol.

distributed evenly among separation, fixed maintenance, and labor, each at around 25%. The feedstock phenol only accounts for less than 10% of the O&M costs because of its low market price. This is in contrast with the case of 1-PE; as shown in Figure 5d, the feedstock (ACP) is the dominant cost driver. In general, the feedstock price and the molecular weight of the products have a large influence on the distribution of the O&M costs in a coupled PEC hydrogenation system.

With the cost distribution identified, we can now determine the economic performance metrics of the various coupled PEC hydrogenation systems considered. The economic metrics NPV, IRR, and EPT for all reactions under base case conditions are listed in Table 2 and Table S8. When no $H_2$-to-chemicals conversion is performed, the resulting NPV is negative, and IRR is not applicable. In this case, the PEC system would never pay for itself over its lifetime. The economic advantages of the coupled hydrogenation reaction become clear as we compare the metrics. For the baseline case of MSA production with a 10% $H_2$-to-MSA conversion efficiency, the NPV of the whole project over 20 years is 1,035 €/m$^2$, and the resulting IRR is 12.4%, which is higher than the 10% hurdle rate set by the H2A default value.[82] An IRR value that is higher than the hurdle rate indicates that the project is worth investing in. In this case, the total investment into the coupled PEC hydrogenation system can be paid back in 13.7 years. Since our current system boundaries do not yet consider factors such as marketing and administration costs, the actual IRR is expected to be somewhat lower but still well above 10%. The numbers for PEC water splitting also show

**Table 2. Net Present Value (NPV), Internal Rate of Return (IRR), and Payback Time (PBT) for the PEC Systems That Include Coupled Hydrogenation Reactions under the Base Case Condition and 10% $H_2$-to-Chemicals Conversion**[a]

| Coupled hydrogenation reactions | $H_2$-to-chemicals conversion | NPV (€/m$^2$) | IRR | PBT (years) |
|---|---|---|---|---|
| Itaconic acid to methylsuccinic acid | 10% | 1035 | 12.4% | 13.7 |
| Levulinic acid to valeric acid | 10% | −874 | | |
| Levulinic acid to γ-valerolactone | 10% | −823 | | |
| Phenol to cyclohexanol | 10% | 812 | 10.5% | 12.4 |
| Acetophenone to 1-phenylethanol | 10% | 21147 | 104.7% | 4.3 |
| Carbon dioxide to ethylene | 10% | −782 | | |
| Carbon dioxide to oxalic acid | 10% | −1062 | | |
| No hydrogenation (i.e., only $H_2$) | | −727 | NA | NA |

[a]Results obtained for other $H_2$-to-chemicals conversion values are shown in Table S8.

significant improvement when coupling it to $H_2$-to-cyclohexanol conversion or $H_2$-to-1-phenylethanol conversion also show outstanding improvement when they are coupled with PEC system. Interestingly, even if the NPV of the cyclohexanol system is lower than that of MSA, the payback time is much shorter. This is because of the greater price difference between the feedstock and the selling price of the product, which results


https://doi.org/10.1021/acssuschemeng.4c03463
ACS Sustainable Chem. Eng. 2024, 12, 13783−13797

in a higher annual revenue. The coupled PEC hydrogenation system that generates 1-phenylethanol is the most profitable one with an IRR of more than 100% and a payback time of less than 5 years for all cases. Finally, coupled PEC hydrogenation of levulinic acid and $CO_2$ (irrespective of the products) are not profitable (negative NPVs), which is attributed to the relatively low market price of products and the low molar mass (for the $CO_2$-derived products). These coupled hydrogenation systems are, therefore, no longer considered in the remainder of our discussions.

The influence of STH efficiencies and lifetime to the resulting LCOH of the various coupled PEC hydrogenation systems will now being discussed. Four additional cases with varying STH efficiency and lifetime are considered in addition to the base case, as shown in Table 3. Figure 6 shows the correlation between LCOH and $H_2$-to-chemicals conversion for all of these cases. When $H_2$ is the only product, i.e., the $H_2$-to-chemicals conversion is zero, the LCOH ranges from 16.6 to 89.3 €/kg. After coupling the PEC system to the more profitable hydrogenation reactions, the LCOH can be reduced to 0 €/kg upon reaching a certain $H_2$-to-chemicals conversion threshold since the revenue of the valorized chemical products is used to compensate the cost of the STH process. We define the cost of SMR-produced $H_2$ as a competitive benchmark (1.4 €/kg, see horizontal yellow dashed lines in Figure 6); the $H_2$-to-chemicals conversion that would result in the LCOH of 1.4 €/kg can therefore be described as the benchmark conversion value (BCV; note that we deliberately avoid the word "efficiency" to avoid confusion with the (different) concept of the energy conversion efficiency). For example, when the PEC system is coupled with the hydrogenation of IA to MSA, even under the least optimal conditions (Case 1), the BCV is 0.55 (intercept between the curve and the horizontal yellow dashed line). Considering that the current maximum $H_2$-to-MSA conversion efficiency demonstrated thus far in the laboratory is 60%, it is expected that this BCV is a realistic target. Lower BCV values are obtained with increasing STH efficiency and lifetime. Figure 6 furthermore reveals that introducing coupled hydrogenation of phenol to cyclohexanol and ACP to 1-PE leads to lower BCVs and is therefore more attractive than the IA-to-MSA process.

The dependence of the LCOH on the market prices of the hydrogenation products is illustrated in Figure 7, which assumes a fixed $H_2$-to-chemicals conversion of 10%. The intersects between the curves and the yellow horizontal dashed lines represent the minimum selling prices of the different coupled hydrogenation products to compete with the benchmark SMR LCOH. The steep vertical slopes of the LCOH in these regions indicate that it is highly sensitive to slight market price changes of the coupled hydrogenation products. The

**Table 3. Solar-to-Hydrogen (STH) Efficiencies and Lifetimes Are Assumed in the Various Cases Considered in This Study**

| | STH | Lifetime |
|---|---|---|
| Case 1 | 5% | 5 |
| Case 2 | 5% | 10 |
| Case 3 | 10% | 5 |
| Case 4 | 10% | 10 |
| Base case | 10% | 20 |

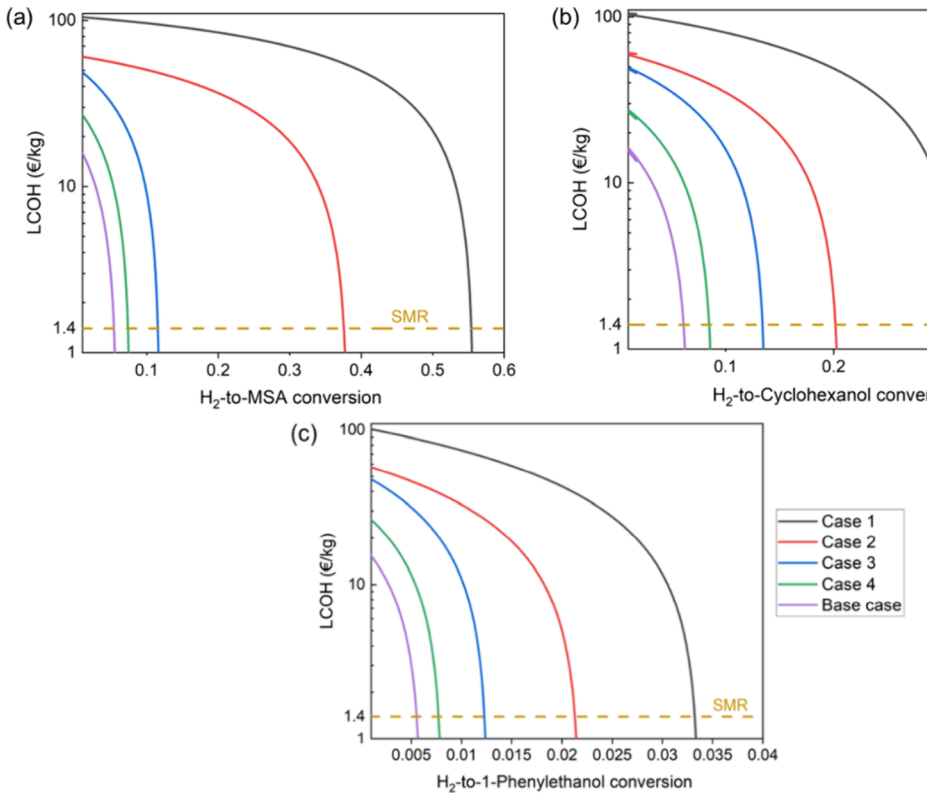


**Figure 6.** Levelized cost of hydrogen (LCOH) as a function of the $H_2$-to-chemicals conversion in coupled PEC hydrogenation of (a) itaconic acid to methyl succinic acid, (b) phenol to cyclohexanol, and (c) acetophenone to 1-phenylethanol. The different cases of STH and lifetime (see Table 3) are considered. Current LCOH from steam methane reforming (SMR) is indicated in each panel as a yellow horizontal dashed lines.



https://doi.org/10.1021/acssuschemeng.4c03463
ACS Sustainable Chem. Eng. 2024, 12, 13783−13797

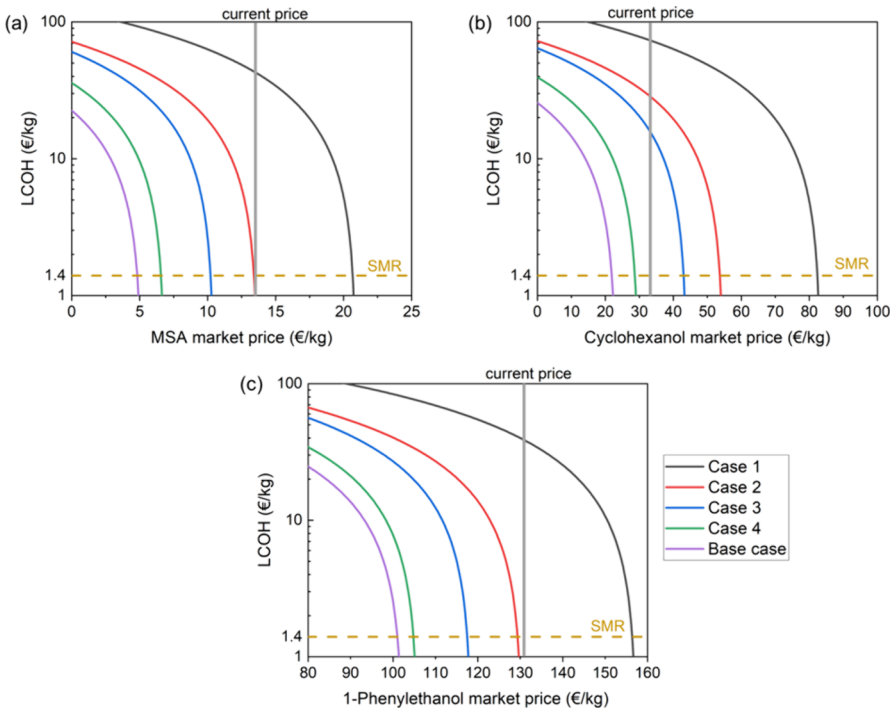


**Figure 7.** Levelized cost of hydrogen (LCOH) as a function of the hydrogenation products market price in coupled PEC hydrogenation of (a) itaconic acid to methyl succinic acid, (b) phenol to cyclohexanol, and (c) acetophenone to 1-phenylethanol. The different cases of STH and lifetime (see Table 3) are considered. The current market prices of each hydrogenation product are indicated as gray vertical lines. The current LCOH from steam methane reforming (SMR) is indicated in each panel as yellow horizontal dashed lines.

current market prices of the products are also indicated as black vertical dashed lines. For the base case conditions, competitive LCOH values vs SMR-produced $H_2$ can be obtained when the selling prices are 4.8, 22, and 101 €/kg for MSA, cyclohexanol, and 1-phenylethanol, respectively. The differences between these prices with the current ones therefore represent the allowable market price fluctuations that could still occur before the respective coupled PEC hydrogenation systems become noncompetitive. This "buffer" ranges become narrower with decreasing STH and lifetime (i.e., from best to worst cases) and ultimately become noncompetitive. Several examples of systems with non-profitable coupled hydrogenation reactions are shown in Figure S3. For these systems, the differences between the current market prices (vertical reference lines) and the competitive market prices (intersects between curves and yellow horizontal dashed lines) illustrate the price increase that must occur before the system can be considered competitive. It is noted that for the coupled PEC hydrogenation of $CO_2$-to-ethylene, the required market price to reach a competitive level would be extremely high (~100 times the current market price, even beyond the range plotted). As such, this reaction should not be considered for coupled PEC hydrogenation systems.

As shown in the cost breakdown section, the cost of the coupled PEC hydrogenation system is driven by the component investment and system parameters, while the revenue is based on sales volume and market price. We perform a sensitivity analysis that varies selected factors by assuming low, base, and high cases and determine their impacts on the most important economic performance indicator, which is the LCOH. We only discuss the coupled PEC $H_2$-to-MSA systems, as the trend is expected to be the same for the other systems. The assumptions defining the low, base, and high cases for this sensitivity analysis are shown in Table S9 for the $H_2$-to-MSA reaction.

Figure 8 shows the results of our sensitivity analysis as a tornado plot. The center point of the plot is the LCOH of 9.83

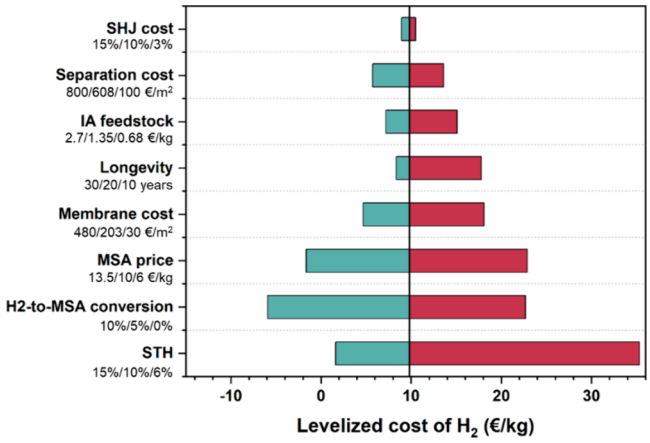


**Figure 8.** Perturbative sensitivity analysis of the LCOH, with lower, base, and higher cases.

€/kg based on the base case assumptions for fabrication and materials, a STH efficiency of 10%, a device longevity of 20 years, and a $H_2$-to-MSA conversion efficiency of 10%. The LCOH is found to be most sensitive to the $H_2$-to-MSA conversion efficiency; a 5% increase in $H_2$-to-MSA conversion efficiency leads to a 160% reduction in LCOH. The selling price of MSA also generates a >100% reduction in LCOH when it is increased from 10 to 13.5 €/kg. An increase in STH efficiency from 5% to 10% would also be highly beneficial and lead to an 83% decrease of the LCOH. In terms of investment


https://doi.org/10.1021/acssuschemeng.4c03463
ACS Sustainable Chem. Eng. 2024, 12, 13783−13797

into the system operation, a ∼ 7-fold reduction in membrane cost and a 35% reduction in separation cost would reduce the LCOH by 52% and 42%, respectively. Finally, our analysis shows that the price of IA feedstock, lifetime, and cost of SHJ cell have a relatively limited influence on the LCOH.

To evaluate the possible impact of the proposed coupled PEC hydrogenation system, we also performed a market analysis for the three hydrogenation products that are shown to be profitable: MSA, cyclohexanol, and 1-phenylethanol. MSA is a valuable chemical compound that finds applications as a cosmetically medium for improving the solubility of lipophilic active agent.[14] MSA is also utilized in the production of a chiral 2,5-dimethyladipic acid diester for polymer synthesis[15] and binder for powder coating.[16] Currently, the market demand for MSA is quite limited. To the best of our knowledge, a market report is not readily available for MSA, but our previous study estimated the annual market demand for MSA to be 15,322 t.[17] With the estimated market price of 13.5 €/kg, the annual market size of MSA is valued at ∼€206 million.

Cyclohexanol is commonly used as a precursor in the production of various chemicals and materials. One of its main uses is as a feedstock in the synthesis of nylon, specifically nylon-6, which is used in the production of fibers, plastics, and other materials. Cyclohexanol is oxidized to cyclohexanone, which is then used as a starting material for the synthesis of adipic acid, a key precursor in nylon-6 production. Cyclohexanol also finds use as a solvent in certain chemical reactions and as a component in perfumes and fragrances. The global cyclohexanol market size was valued at US$ 7.95 billion in 2022 and is expected to expand at a compound annual growth rate (CAGR) of 4.58% during the forecast period, reaching US $ 10.4 billion by 2028.[83] Based on the current market price, this leads to a market demand of ∼240,000 t per year.

1-Phenylethanol finds versatile applications in the fragrance and flavor industries, where it contributes to the production of perfumes, cosmetics, and scented products. It is also used as a flavoring agent in foods and beverages, offering a distinct floral taste. Additionally, its antimicrobial properties make it potentially valuable in pharmaceutical formulations. As a synthetic building block, 1-phenylethanol is employed in chemical syntheses, and its solvent properties further extend its utility. The global 1-phenylethanol market was valued at US$ 491.7 million in 2021 and is projected to reach US$ 761.7 million by 2031, growing at a CAGR of 3.3% from 2022 to 2031.[84] This translates to a total market demand of 5,814.5 t per year.

We now compare the market demand for the three hydrogenation products discussed above to that for hydrogen. According to the International Energy Agency (IEA), the global $H_2$ market demand was 150 million tons (Mt) in 2023 and is projected to increase to over 500 Mt by 2050.[85] Assuming that the coupled PEC hydrogenation systems have 10% $H_2$-to-chemicals conversion, we calculate the corresponding annual $H_2$ production if the total annual demand of each hydrogenation product is met. The results are shown in Table S10. Coupled PEC hydrogenation to the cyclohexanol system could potentially contribute to ∼0.1% of total global $H_2$ demand, while the 1-phenylethanol system could only contribute to ∼0.0006% of the global $H_2$ demand. This is interesting because, although we have shown in the previous section that coupled PEC hydrogenation systems generating 1-phenylethanol would have the highest economic profitability, its impact on the global $H_2$ market is minimal due to its relatively small market demand. Our analysis also illustrates that the market sizes of the hydrogenation reactions considered here are orders of magnitude lower than that of $H_2$. Hydrogenation reactions with larger market sizes need to be explored for the coupled PEC hydrogenation concept to reach its desired impact. It should also be noted that the flexibility of the coupled PEC concept also allows for multiple hydrogenation reactions within the same system.

## CONCLUSIONS

In summary, we have conducted a comprehensive techno-economic assessment (TEA) of a coupled PEC hydrogenation facility based on our recent demonstrated device,[13,17,45] assuming a 1,000 kg $H_2$/day capacity. Seven potential hydrogenation reactions were considered based on their reported reaction conditions that are close to that of PEC device (i.e., room temperature, atmospheric pressure). These reactions include IA to MSA, levulinic acid to valeric acid, and γ-valerolactone, phenol to cyclohexanol, acetophenone (ACP) to 1-phenyl ethanol (1-PE), and $CO_2$ to ethylene and oxalic acid. Our life cycle inventories of the system revealed that the PEC reactor is the major contributor to the capital cost, with the membrane (Nafion) being the most expensive component. Feedstock cost and product separation were identified as the largest O&M cost components. Under the base case scenario of 10% STH efficiency and 20 year lifetime, the system net present value (NPV) and internal rate of return (IRR) are negative when $H_2$ is the only product, i.e., no coupled hydrogenation, indicating that the system is not capable of generating adequate payback. The NPV and IRR become positive when coupled hydrogenation of IA to MSA, phenol to cyclohexanol, and ACP to 1-PE were introduced, even with a relatively low $H_2$-to-chemicals conversion of 10%. Coupled hydrogenation of ACP to 1-PE were identified as the one generating the highest values, although the potential market impact of cyclohexanol is the largest among the three reactions. Introducing the other coupled hydrogenation reactions is not favorable because of the relatively low yielding or market price of the products. Sensitivity analysis shows that solar-to-$H_2$ efficiency and $H_2$-to-chemicals conversion are the most critical parameters affecting the LCOH of the system. Even under the worst-case scenario considered here (STH 5%, lifetime 5 years), the required benchmark conversions that would result in competitive LCOH values that are comparable to that of fossil fuel-based $H_2$ are 55.4%, 31.9%, and 9.5% for coupled IA-to-MSA, phenol-to-cyclohexanol and ACP-to-1-PE systems, respectively. These are lower than those already reported in our coupled PEC hydrogenation of IA-to-MSA demonstration device, suggesting the feasibility of fulfilling these benchmark values. Overall, our study highlights the economic benefits and further supports the attractiveness of coupling hydrogenation reactions inside a PEC $H_2$ generation system.

Finally, while the current state of PEC water-splitting technology demonstrates promising advancements, significant challenges remain before it can be commercially deployed on a large scale.[86] Economically, the current study indicates that the integration of chemical synthesis offers a pathway for PEC to compete with other hydrogen production methods, such as steam methane reforming. However, technically, the largest demonstration of deployed large-scale PEC devices being built and test to date is still limited, including a 200 $cm^2$ modular cell (with multiple 50 $cm^2$ single-large α-$Fe_2O_3$ photoelectrodes) that can reach 0.41% STH under concentrated


https://doi.org/10.1021/acssuschemeng.4c03463
ACS Sustainable Chem. Eng. 2024, 12, 13783−13797

sunlight and 1.6 $m^2$ Artiphyction prototype (with 100 PEC cells of 8 × 8 $cm^2$ CoPi-catalyzed Mo-doped $BiVO_4$ photoanode) that can reach 3% STH efficiency.[87,88] Thus, continued research is essential to further enhance the long-term stability and efficiency of the large-area PEC technology.

## ■ ASSOCIATED CONTENT

### Supporting Information

The Supporting Information is available free of charge at https://pubs.acs.org/doi/10.1021/acssuschemeng.4c03463.

Reported LCOH for different hydrogen production technologies, chemical structures and market prices of feedstocks and products, base case parameters of the TEA, life cycle inventory data used in the TEA, additional economic metrics data, assumptions used in the sensitivity analysis, market analysis data, schematic diagram of the separation process considered, capital cost breakdown of only $H_2$-producing system, LCOH data for less profitable coupled PEC hydrogenation reactions (PDF)

## ■ AUTHOR INFORMATION


### Corresponding Author

**Fatwa F. Abdi** − *School of Energy and Environment, City University of Hong Kong, Kowloon, Hong Kong S.A.R., China; Institute for Solar Fuels, Helmholtz-Zentrum Berlin für Materialien und Energie GmbH, Berlin 14109, Germany;* orcid.org/0000-0001-5631-0620; Email: ffabdi@cityu.edu.hk

### Authors

**Xinyi Zhang** − *School of Energy and Environment, City University of Hong Kong, Kowloon, Hong Kong S.A.R., China; Institute for Solar Fuels, Helmholtz-Zentrum Berlin für Materialien und Energie GmbH, Berlin 14109, Germany; Technische Universität Berlin, Department of Chemistry, Berlin 10623, Germany*

**Zishuo Li** − *Technische Universität Berlin, Department of Chemistry, Berlin 10623, Germany*

**Lasfitri Rosanty Sinaga** − *Hochschule für Technik und Wirtschaft Berlin, University of Applied Science, School of Engineering − Technology and Life, Berlin 10318, Germany*

**Michael Schwarze** − *Technische Universität Berlin, Department of Chemistry, Berlin 10623, Germany*

**Reinhard Schomäcker** − *Technische Universität Berlin, Department of Chemistry, Berlin 10623, Germany;* orcid.org/0000-0003-3106-3904

**Roel van de Krol** − *Institute for Solar Fuels, Helmholtz-Zentrum Berlin für Materialien und Energie GmbH, Berlin 14109, Germany; Technische Universität Berlin, Department of Chemistry, Berlin 10623, Germany;* orcid.org/0000-0003-4399-399X

Complete contact information is available at: https://pubs.acs.org/10.1021/acssuschemeng.4c03463


### Notes

The authors declare no competing financial interest.

## ■ ACKNOWLEDGMENTS

All authors acknowledge support from the Deutsche Forschungsgemeinschaft (DFG, German Research Foundation) under Germany's Excellence Strategy—EXC 2008/1 (UniSysCat)—390540038 and from the German Helmholtz Association—Excellence Network—ExNet-0024-Phase2-3. X.Z. and F.F.A. acknowledge support from CityU (project 9610621).

## ■ REFERENCES


(1) United Nations. Paris Agreement, 2024. https://www.un.org/en/climatechange/paris-agreement (accessed 2024−01).

(2) Hydrogen Council. *How hydrogen empowers the energy transition*, 2017. https://hydrogencouncil.com/en/study-how-hydrogen-empowers.

(3) International Energy Agency. IEA Global Hydrogen Review 2023, 2023. https://www.iea.org/reports/global-hydrogen-review-2023.

(4) IEA. Future of Hydrogen: Seizing today's opportunities, 2019. https://www.iea.org/reports/the-future-of-hydrogen.

(5) Yang, W.; Park, J.; Kwon, H.-C.; Hutter, O. S.; Phillips, L. J.; Tan, J.; Lee, H.; Lee, J.; Tilley, S. D.; Major, J. D.; Moon, J. Solar water splitting exceeding 10% efficiency via low-cost $Sb_2Se_3$ photocathodes coupled with semitransparent perovskite photovoltaics. *Energy Environ. Sci.* **2020**, *13* (11), 4362−4370.

(6) Cheng, W.-H.; Richter, M. H.; May, M. M.; Ohlmann, J.; Lackner, D.; Dimroth, F.; Hannappel, T.; Atwater, H. A.; Lewerenz, H.-J. Monolithic Photoelectrochemical Device for Direct Water Splitting with 19% Efficiency. *ACS Energy Lett.* **2018**, *3* (8), 1795−1800.

(7) van de Krol, R.; Parkinson, B. A. Perspectives on the photoelectrochemical storage of solar energy. *MRS Energy & Sustainability* **2017**, *4*, No. E13.

(8) Pinaud, B. A.; Benck, J. D.; Seitz, L. C.; Forman, A. J.; Chen, Z.; Deutsch, T. G.; James, B. D.; Baum, K. N.; Baum, G. N.; Ardo, S.; et al. Technical and economic feasibility of centralized facilities for solar hydrogen production via photocatalysis and photoelectrochemistry. *Energy Environ. Sci.* **2013**, *6* (7), 1983−2002.

(9) Shaner, M. R.; Atwater, H. A.; Lewis, N. S.; McFarland, E. W. A comparative technoeconomic analysis of renewable hydrogen production using solar energy. *Energy Environ. Sci.* **2016**, *9* (7), 2354−2371.

(10) Acar, C.; Dincer, I. Comparative assessment of hydrogen production methods from renewable and non-renewable sources. *Int. J. Hydrogen Energy* **2014**, *39* (1), 1−12.

(11) Conventional hydrogen yields slightly. *Hydex weekly report*, 2022. https://www.energate-messenger.com/news/222655/conventional-hydrogen-yields-slightly (accessed 2023−06).

(12) Glenk, G.; Reichelstein, S. Economics of converting renewable power to hydrogen. *Nature Energy* **2019**, *4* (3), 216−222.

(13) Obata, K.; Schwarze, M.; Thiel, T. A.; Zhang, X.; Radhakrishnan, B.; Ahmet, I. Y.; van de Krol, R.; Schomäcker, R.; Abdi, F. F. Solar-driven upgrading of biomass by coupled hydrogenation using in situ (photo)electrochemically generated $H_2$. *Nat. Commun.* **2023**, *14*, 6017.

(14) Richard, H.; Muller, B. Use of a 2-methylsuccinic acid diester derivative as solvent in cosmetic compositions. EP2683351A2, 2016.

(15) Wu, L.; Mascal, M.; Farmer, T.; Arnaud, P. C.; Chang, M. W. Electrochemical Coupling of Biomass-derived Carboxylic Acids: C8 Platforms for Renewable Polymers and Fuels. *ChemSusChem* **2017**, *10*, 166.

(16) Darijo, M.; Jozsef, S. Z.; Jens, H.; Sebastien, G. Powder coating useful as a coating agent, and for coating metallic- and non-metallic surfaces, comprises a binder comprising methyl succinic acid. DE102011080722A1, 2011.

(17) Zhang, X.; Schwarze, M.; Schomäcker, R.; van de Krol, R.; Abdi, F. F. Life cycle net energy assessment of sustainable $H_2$ production and hydrogenation of chemicals in a coupled photoelectrochemical device. *Nat. Commun.* **2023**, *14* (1), 991.

(18) Nieder-Heitmann, M.; Haigh, K. F.; Görgens, J. F. Life cycle assessment and multi-criteria analysis of sugarcane biorefinery

scenarios: Finding a sustainable solution for the South African sugar industry. *Journal of Cleaner Production* **2019**, *239*, 118039.
(19) Hayes, G. C.; Becer, C. R. Levulinic acid: A sustainable platform chemical for novel polymer architectures. *Polym. Chem.* **2020**, *11* (25), 4068−4077.
(20) Yan, J.; Meng, Q.; Shen, X.; Chen, B.; Sun, Y.; Xiang, J.; Liu, H.; Han, B. Selective valorization of lignin to phenol by direct transformation of Csp2−Csp3 and C−O bonds. *Science Advances* **2020**, *6* (45), No. eabd1951.
(21) Kloetzer, L.; Petrila-Cocuz, I.-B.; Galaction, A.-I.; Szita, N.; Blaga, A.-C.; Cascaval, D. Eco-friendly production of chemicals 1. improvement of enzymatic production of acetophenone by direct extraction. *Environmental Engineering and Management Journal* **2016**, *15* (8), 1849−1854.
(22) Holzhäuser, F. J.; Artz, J.; Palkovits, S.; Kreyenschulte, D.; Büchs, J.; Palkovits, R. Electrocatalytic upgrading of itaconic acid to methylsuccinic acid using fermentation broth as a substrate solution. *Green Chem.* **2017**, *19* (10), 2390−2397.
(23) Akhade, S. A.; Singh, N.; Gutiérrez, O. Y.; Lopez-Ruiz, J.; Wang, H.; Holladay, J. D.; Liu, Y.; Karkamkar, A.; Weber, R. S.; Padmaperuma, A. B.; et al. Electrocatalytic hydrogenation of biomass-derived organics: a review. *Chem. Rev.* **2020**, *120* (20), 11370−11419.
(24) Xin, L.; Zhang, Z.; Qi, J.; Chadderdon, D. J.; Qiu, Y.; Warsko, K. M.; Li, W. Electricity Storage in Biofuels: Selective Electrocatalytic Reduction of Levulinic Acid to Valeric Acid or γ-Valerolactone. *ChemSusChem* **2013**, *6* (4), 674−686.
(25) Yan, K.; Yang, Y.; Chai, J.; Lu, Y. Catalytic reactions of gamma-valerolactone: A platform to fuels and value-added chemicals. *Applied Catalysis B: Environmental* **2015**, *179*, 292−304.
(26) Sudhakar, M.; Lakshmi Kantam, M.; Swarna Jaya, V.; Kishore, R.; Ramanujachary, K.V.; Venugopal, A. Hydroxyapatite as a novel support for Ru in the hydrogenation of levulinic acid to γ-valerolactone. *Catal. Commun.* **2014**, *50*, 101−104.
(27) Song, Y.; Chia, S. H.; Sanyal, U.; Gutiérrez, O. Y.; Lercher, J. A. Integrated catalytic and electrocatalytic conversion of substituted phenols and diaryl ethers. *J. Catal.* **2016**, *344*, 263−272.
(28) Villalba, M.; del Pozo, M.; Calvo, E. J. Electrocatalytic hydrogenation of acetophenone and benzophenone using palladium electrodes. *Electrochim. Acta* **2015**, *164*, 125−131.
(29) Nitopi, S.; Bertheussen, E.; Scott, S. B.; Liu, X.; Engstfeld, A. K.; Horch, S.; Seger, B.; Stephens, I. E.; Chan, K.; Hahn, C.; et al. Progress and perspectives of electrochemical $CO_2$ reduction on copper in aqueous electrolyte. *Chem. Rev.* **2019**, *119* (12), 7610−7672.
(30) Mistry, H.; Varela, A. S.; Bonifacio, C. S.; Zegkinoglou, I.; Sinev, I.; Choi, Y.-W.; Kisslinger, K.; Stach, E. A.; Yang, J. C.; Strasser, P.; et al. Highly selective plasma-activated copper catalysts for carbon dioxide reduction to ethylene. *Nat. Commun.* **2016**, *7* (1), 12123.
(31) Boor, V.; Frijns, J. E.; Perez-Gallent, E.; Giling, E.; Laitinen, A. T.; Goetheer, E. L.; Van Den Broeke, L. J.; Kortlever, R.; De Jong, W.; Moultos, O. A.; et al. Electrochemical reduction of $CO_2$ to oxalic acid: experiments, process modeling, and economics. *Ind. Eng. Chem. Res.* **2022**, *61* (40), 14837−14846.
(32) Zimmermann, A.; Müller, L.; Wang, Y.; Langhorst, T.; Wunderlich, J.; Marxen, A.; Armstrong, K.; Buchner, G.; Kätelhön, A.; Bachmann, M. Techno-Economic Assessment & Life Cycle Assessment Guidelines for $CO_2$ Utilization (Version 1.1), 2020. DOI: 10.3998/2027.42/162573.
(33) James, B. D.; Baum, G. N.; Perez, J.; Baum, K. N. Technoeconomic analysis of photoelectrochemical (PEC) hydrogen production. DOE Report, Directed Tecnologies, 2009. https://www1.eere.energy.gov/hydrogenandfuelcells/pdfs/pec_technoeconomic_analysis.pdf.
(34) Deutscher Wetterdienst. Global, diffuse and direct radiation (monthly and annual totals and deviations), 2022. https://www.dwd.de/EN/ourservices/solarenergy/maps_globalradiation_sum_new.html (accessed 2024−01).
(35) Huld, T.; Müller, R.; Gambardella, A. A new solar radiation database for estimating PV performance in Europe and Africa. *Sol. Energy* **2012**, *86* (6), 1803−1815.
(36) KITCO. Platinum spot price, 2022. https://www.kitco.com/charts/interactive-charts/?Symbol=PLATINUM&Currency=USD&multiCurrency=true&langId=EN&period=2329200000&utm_source=kitco&utm_medium=banner&utm_content=20110407_iCharts_182day_platinum_link&utm_campaign=iCharts (accessed 2024−01).
(37) Public Net Electricity Generation 2023 in Germany: Renewables Cover the Majority of the Electricity Consumption for the First Time, *Fraunhofer Institute for Solar Energy System ISE*, 2024. https://www.ise.fraunhofer.de/en/press-media/press-releases/2024/public-electricity-generation-2023-renewable-energies-cover-the-majority-of-german-electricity-consumption-for-the-first-time.html. (accessed 2024 −01).
(38) Deutsche Bundesbank Eurosystem. Expected real interest rates. 2023. https://www.bundesbank.de/en/statistics/money-and-capital-markets/interest-rates-and-yields/expected-real-interest-rates/expected-real-interest-rates-793666 (accessed 2023−06).
(39) Collins, L. Green hydrogen now cheaper to produce than grey $H_2$ across Europe due to high fossil gas prices, 2021. https://www.rechargenews.com/energy-transition/green-hydrogen-now-cheaper-to-produce-than-grey-h2-across-europe-due-to-high-fossil-gas-prices/2-1-1098104 (accessed 2024 −01).
(40) Petrova, V. H2V Energies to build green hydrogen plant in Quebec, opens order book, 2020. https://renewablesnow.com/news/h2v-energies-to-build-green-hydrogen-plant-in-quebec-opens-order-book-684374/ (accessed 2024−01).
(41) Collins, L. Green hydrogen' on sale in open market at 80% higher price than grey $H_2$, 2020. https://www.rechargenews.com/transition/green-hydrogen-on-sale-in-open-market-at-80-higher-price-than-grey-h2/2-1-743348 (accessed 2024−01).
(42) H2V Energies. Production of green hydrogen Value chain - Bécancour plant, 2023. https://www.h2venergies.com/secteurs-dactivite (accessed 2023−06).
(43) Alfa Aesar. Methylsuccinic acid, 99%, 2022. https://www.thermofisher.com/order/catalog/product/H60967.22 (accessed 2024−01).
(44) Sigma-Aldrich. Methylsuccinic acid, 2022. https://www.sigmaaldrich.com/DE/en/product/aldrich/m81209 (accessed 2024−01).
(45) Obata, K.; Schwarze, M.; Thiel, T. A.; Zhang, X.; Radhakrishnan, B.; Ahmet, I. Y.; van de Krol, R.; Schomäcker, R.; Abdi, F. F. Solar-driven upgrading of biomass-derived feedstock by coupled homogeneous hydrogenation using in-situ (photo)-electrochemically generated $H_2$. *Nat. Commun.* **2023**, *14*, 6017.
(46) WallStreetPrep. Internal Rate of Return (IRR), 2023. https://www.wallstreetprep.com/knowledge/irr-internal-rate-of-return/ (accessed 2024−01).
(47) Wenderich, K.; Kwak, W.; Grimm, A.; Kramer, G. J.; Mul, G.; Mei, B. Industrial feasibility of anodic hydrogen peroxide production through photoelectrochemical water splitting: a techno-economic analysis. *Sustainable Energy & Fuels* **2020**, *4* (6), 3143−3156.
(48) Sathre, R.; Scown, C. D.; Morrow, W. R.; Stevens, J. C.; Sharp, I. D.; Ager, J. W.; Walczak, K.; Houle, F. A.; Greenblatt, J. B. Life-cycle net energy assessment of large-scale hydrogen production via photoelectrochemical water splitting. *Energy Environ. Sci.* **2014**, *7* (10), 3264−3278.
(49) Fehr, A. M.; Deutsch, T. G.; Toma, F. M.; Wong, M. S.; Mohite, A. D. Technoeconomic Model and Pathway to< $2/kg Green Hydrogen Using Integrated Halide Perovskite Photoelectrochemical Cells. *ACS Energy Letters* **2023**, *8* (12), 4976−4983.
(50) Ahmet, I. Y.; Ma, Y.; Jang, J.-W.; Henschel, T.; Stannowski, B.; Lopes, T.; Vilanova, A.; Mendes, A.; Abdi, F. F.; van de Krol, R. Demonstration of a 50 $cm^2$ $BiVO_4$ tandem photoelectrochemical-photovoltaic water splitting device. *Sustainable Energy & Fuels* **2019**, *3* (9), 2366−2379.

(51) Ko, Y.-S.; Kwon, Y.-U. Electrochemical deposition of platinum on fluorine-doped tin oxide: The nucleation mechanisms. *Electrochim. Acta* **2010**, *55* (24), 7276−7281.
(52) Zhai, P.; Haussener, S.; Ager, J.; Sathre, R.; Walczak, K.; Greenblatt, J.; McKone, T. Net primary energy balance of a solar-driven photoelectrochemical water-splitting device. *Energy Environ. Sci.* **2013**, *6* (8), 2380−2389.
(53) Kuang, Y.; Jia, Q.; Ma, G.; Hisatomi, T.; Minegishi, T.; Nishiyama, H.; Nakabayashi, M.; Shibata, N.; Yamada, T.; Kudo, A.; et al. Ultrastable low-bias water splitting photoanodes via photocorrosion inhibition and in situ catalyst regeneration. *Nat. Energy* **2017**, *2* (1), 16191.
(54) Liu, Z.; Peters, M.; Shanmugam, V.; Khoo, Y. S.; Guo, S.; Stangl, R.; Aberle, A. G.; Wong, J. Luminescence imaging analysis of light harvesting from inactive areas in crystalline silicon PV modules. *Sol. Energy Mater. Sol. Cells* **2016**, *144*, 523−531.
(55) Colella, W. G.; James, B.; Moton, J. M. Hydrogen Pathways Analysis for Polymer Electrolyte Membrane (PEM) Electrolysis. *2014 DOE Hydrogen and Fuel Cells Program and Vehicle Technologies Office Annual Merit Review and Peer Evaluation Meeting*, Project ID: PD102, 2014.
(56) Germany engineer salary: How much do engineers earn?, 2024. https://www.academics.com/guide/engineer-salary-germany (accessed 2024 26 Feb).
(57) DEG Press Office. DEG finances solar power plant in South Africa, 2019. https://www.deginvest.de/Newsroom/News/Pressemitteilungen-Details_515840-2.html (accessed 2024 26 Feb).
(58) Berliner Wasserbetriebe. Our Tariffs for Drinking Water and Drainage, 2022. https://www.bwb.de/en/1720.php (accessed 2024−01).
(59) Koptyug, E. Annual electricity prices (including electricity tax) for industrial businesses in Germany from 1998 to 2024, 2022. https://www.statista.com/statistics/1050448/industrial-electricity-prices-including-tax-germany (accessed 2024−01).
(60) Louwen, A.; Van Sark, W.; Schropp, R.; Faaij, A. A cost roadmap for silicon heterojunction solar cells. *Sol. Energy Mater. Sol. Cells* **2016**, *147*, 295−314.
(61) Abdi, F. F.; van de Krol, R. Nature and light dependence of bulk recombination in Co-Pi-catalyzed BiVO4 photoanodes. *J. Phys. Chem. C* **2012**, *116* (17), 9398−9404.
(62) Sánchez-Cruces, E.; Barrera-Calva, E.; Lavanderos, K.; González, F. Life cycle analysis (LCA) of solar selective thin films by electrodeposition and by sol-gel techniques. *Energy Procedia* **2014**, *57*, 2812−2818.
(63) Zhai, P.; Williams, E. D. Dynamic hybrid life cycle assessment of energy and carbon of multicrystalline silicon photovoltaic systems. *Environ. Sci. Technol.* **2010**, *44* (20), 7950−7955.
(64) Kim, H.; Fthenakis, V. Comparative life-cycle energy payback analysis of multi-junction a-SiGe and nanocrystalline/a-Si modules. *Progress in Photovoltaics: Research and Applications* **2011**, *19* (2), 228−239.
(65) Alsema, E. Energy requirements of thin-film solar cell modules–a review. *Renewable Sustainable Energy Rev.* **1998**, *2*, 387.
(66) Hayter, S.; Tanner, S.; Urbatsch, E.; Zuboy, J. Saving energy, water, and money with efficient water treatment technologies. *US Department of Energy, National Renewable Energy Laboratory (NREL), Federal Energy Managment Program (FEMP)*, 2004. https://research-hub.nrel.gov/en/publications/saving-energy-water-and-money-with-efficient-water-treatment-tech.
(67) Wasserhaus. Platinumwasser NEO-7 Reverse Osmosis System, 2022. https://www.wasserhaus.de/epages/62372559.sf/en_GB/?ViewObjectPath=%2FShops%2F62372559%2FProducts%2F13244 (accessed 2024−01).
(68) Shanmuganathan, S.; Johir, M.; Listowski, A.; Vigneswaran, S.; Kandasamy, J. Sustainable processes for treatment of waste water reverse osmosis concentrate to achieve zero waste discharge: a detailed study in water reclamation plant. *Procedia Environmental Sciences* **2016**, *35*, 930−937.
(69) Macknick, J.; Newmark, R.; Heath, G.; Hallett, K. C. Operational water consumption and withdrawal factors for electricity generating technologies: a review of existing literature. *Environmental Research Letters* **2012**, *7* (4), 045802.
(70) AxFlow. Kreiselpumpe mit Peripherallaufrad, Pedrollo PQ-PRO, 2022. https://www.axflow24.de/home/Kreiselpumpe-mit-Peripherallaufrad-Pedrollo-PQ-PRO-230V-p224372875 (accessed 2024−01).
(71) Plappally, A.K.; Lienhard V, J.H. Energy requirements for water production, treatment, end use, reclamation, and disposal. *Renewable Sustainable Energy Rev.* **2012**, *16* (7), 4818−4848.
(72) National Instruments. What is NI LabVIEW?, 2022. https://www.ni.com/en/shop/labview.html?cid=PSEA-7013q000001fLK5AAM-CONS-GOGSE_161597905120&utm_keyword=labview%20software&gad_source=1&gclid=CjwKCAjwhvi0BhA4EiwAX25ujweGFXV_8dMTB62wjxhEM02nxENb6-adVbrPkkTV5TVrCRx10V_r_xoCG78QAvD_BwE#521715&s_kwcid=AL!6304!3!691563588237!b!!g!!labview%20software (accessed 2024−01).
(73) PLC-Schäfer. Programmable logic controller (PLC): featured products, 2022. https://www.plc-electronic.de/en (accessed 2024−01).
(74) Dell. Desktop-PCs, 2022. https://www.dell.com/de-de/shop/desktops-all-in-ones-pcs/sc/desktops (accessed 2024 −01).
(75) Smith, E.; Morris, J.; Kheshgi, H.; Teletzke, G.; Herzog, H.; Paltsev, S. The cost of $CO_2$ transport and storage in global integrated assessment modeling. *International Journal of Greenhouse Gas Control* **2021**, *109*, 103367.
(76) Meulen, S.; Grijspaardt, T.; Mars, W.; Geest, W.; Roest-Crollius, A.; Kiel, J. *Cost Figures for Freight Transport - Final Report*; Panteia, 2023.
(77) Mettler Toledo. Continuous Stirred Tank Reactors (CSTRs), 2022. https://www.mt.com/de/en/home/applications/L1_AutoChem_Applications/L2_ReactionAnalysis/continuous-stirred-tank-reactor-cstr.cmp.243074089.html?cmp=243074089 (accessed 2024−01).
(78) Pasteurization continuous stirred reactor food grade stainless steel tank. *Nanjing Qiu Rong Machinery Equipment Co., Ltd.*, 2022. https://www.alibaba.com/product-detail/pasteurization-continuous-stirred-reactor-food-grade_60613823908.html (accessed 2024−01).
(79) Efe, Ç.; van der Wielen, L. A.; Straathof, A. J. Techno-economic analysis of succinic acid production using adsorption from fermentation medium. *Biomass and Bioenergy* **2013**, *56*, 479−492.
(80) Wang, H.; Cui, C.; Lyu, H.; Sun, J. Design and economic evaluation of energy-saving industrial distillation processes for separating close-boiling cyclohexanone-cyclohexanol mixture. *Sep. Purif. Technol.* **2019**, *211*, 279−289.
(81) James, B. D.; Huya-Kouadio, J. M.; Houchins, C.; DeSantis, D. A. *Mass Production Cost Estimation of Direct $H_2$ PEM Fuel Cell Systems for Transportation Applications*; US Department of Energy, 2018.
(82) Steward, D.; Ramsden, T.; Zuboy, J. *H2A Production Model, Version 2 User Guide*; Technical Report NREL/TP-560-43983; National Renewable Energy Lab.(NREL), Golden, CO, 2008.
(83) Grandview Research. *Cyclohexanol Market Size, Share & Trends Analysis Report By Product, By Application, By Region, And Segment Forecasts, 2023 to 2030*, 2023. https://www.marketwatch.com/press-release/cyclohexanol-market-2023-2030-new-developments-in-the-industry-2023-06-06 (accessed 2023−08).
(84) Anjumnisha, S.; Narune, A.; Eswara, P. *2-Phenylethanol Market by Type (Natural and Synthetic) and End-use Industry (Food & Beverage, Personal Care & Cosmetics, Pharmaceutical, and Others): Global Opportunity Analysis and Industry Forecast, 2022−2031*, 2023. https://www.alliedmarketresearch.com/2-phenylethanol-market-A17166 (accessed 2024−01).
(85) *Net Zero by 2050: A Roadmap for the Global Energy Sector*; International Energy Agency, 2021.
(86) Vilanova, A.; Dias, P.; Lopes, T.; Mendes, A. The route for commercial photoelectrochemical water splitting: a review of large-

area devices and key upscaling challenges. *Chem. Soc. Rev.* **2024**, *53*, 2388.
(87) Vilanova, A.; Dias, P.; Azevedo, J.; Wullenkord, M.; Spenke, C.; Lopes, T.; Mendes, A. Solar water splitting under natural concentrated sunlight using a 200 $cm^2$ photoelectrochemical-photovoltaic device. *J. Power Sources* **2020**, *454*, 227890.
(88) Tolod, K. R.; Hernández, S.; Russo, N. Recent advances in the $BiVO_4$ photocatalyst for sun-driven water oxidation: top-performing photoanodes and scale-up challenges. *Catalysts* **2017**, *7* (1), 13.



https://doi.org/10.1021/acssuschemeng.4c03463
*ACS Sustainable Chem. Eng.* 2024, 12, 13783−13797